

Discovery and Computational Rationalization of Diminishing Alternation in $[n]$ Dendralenes

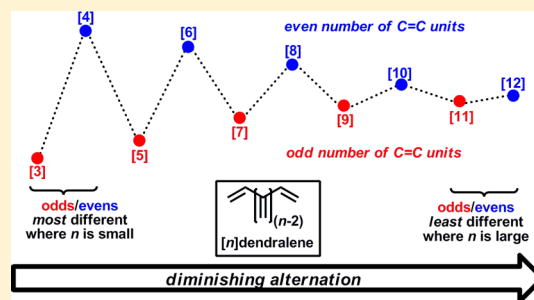
Mehmet F. Saglam,[†] Thomas Fallon,[†] Michael N. Paddon-Row,^{*,‡} and Michael S. Sherburn^{*,†}

[†]Research School of Chemistry, Australian National University, Canberra, Australian Capital Territory 2601, Australia

[‡]School of Chemistry, The University of New South Wales, Sydney, New South Wales 2052, Australia

S Supporting Information

ABSTRACT: The $[n]$ dendralenes are a family of acyclic hydrocarbons which, by virtue of their ability to rapidly generate structural complexity, have attracted significant recent synthetic attention. [3]Dendralene through [8]dendralene have been previously prepared but no higher member of the family has been reported to date. Here, we describe the first chemical syntheses of the “higher” dendralenes, [9]dendralene through [12]dendralene. We also report a detailed investigation into the spectroscopic properties and chemical reactivity of the complete family of fundamental hydrocarbons, [3]dendralene to [12]dendralene. These studies reveal the first case of diminishing alternation in behavior in a series of related structures. We also report a comprehensive series of computational studies, which trace this dampening oscillatory effect in both spectroscopic measurements and chemical reactivity to conformational preferences.



INTRODUCTION

The dendralenes are one of the four fundamental classes of oligo-olefinic hydrocarbon structures comprising exclusively sp^2 -hybridized carbons (Figure 1).^{1,2} The dendralenes are

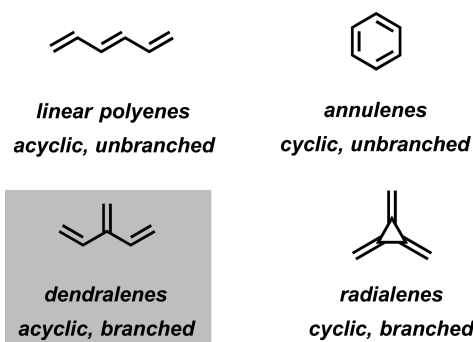


Figure 1. Four fundamental classes of conjugated oligo-alkenes and the family under scrutiny (shaded).

acyclic, branched chain systems; the remaining three families are the “polyenes” (acyclic and unbranched), the radialenes (cyclic and branched) and the annulenes (cyclic and unbranched).³ Until the turn of the century, the dendralenes had received the least attention, most likely due to the erroneous assumption that they were too unstable to be handled in the laboratory using standard equipment and methods. Indeed, only the triene^{4–8} and tetraene^{1a,7–11} were reported prior to 2000.

The radialenes¹² are also relatively poorly investigated, with only the triene,¹³ tetraene,¹⁴ pentaene,¹⁵ and hexaene¹⁶

reported in the literature. In contrast, the unbranched systems have received significant attention, which is unsurprising when the number of natural products containing linear polyenic¹⁷ and annulenic systems¹⁸ is considered. Regarding our understanding of how structure relates to reactivity and stability, the alternating behavior of the planarized annulenes, predicted by Hückel’s rule,¹⁹ is an essential chemistry concept.^{3,20} Thus, the “1,2-ethenologous” series of annulenes, namely 1,3-cyclobutadiene (antiaromatic) → benzene (aromatic) → 1,3,5,7-cyclooctatetraene (antiaromatic) and so forth represents an alternating progression of less and more stable compounds. The physical and chemical properties of the annulenes are dominated by this parity-dependent behavior. Alternations in melting points in families of compounds of even- and odd-length chains has also been reported, a property traced to the packing of molecules in crystal lattices.²¹ In these systems, alternation in behavior does not extend to any other physical or chemical property. In 2009, we reported parity dependent behavior in the $[n]$ dendralenes ($n = 3–8$) (1–6), whereupon we noted that the odd members of the family (1, 3 and 5) are less stable than the even parity members (2, 4 and 6).⁸ Furthermore, in the UV–visible spectra, we observed a linear correlation for the even parity dendralenes in a plot of the extinction coefficient versus the number of C=C units, whereas the odd members showed no such correlation. In addition, the odd parity dendralenes were shown to react as dienes, undergoing relatively clean and site-selective monocycloadditions on exposure to 1 mol equiv of the electron poor

Received: November 23, 2015

Published: December 31, 2015

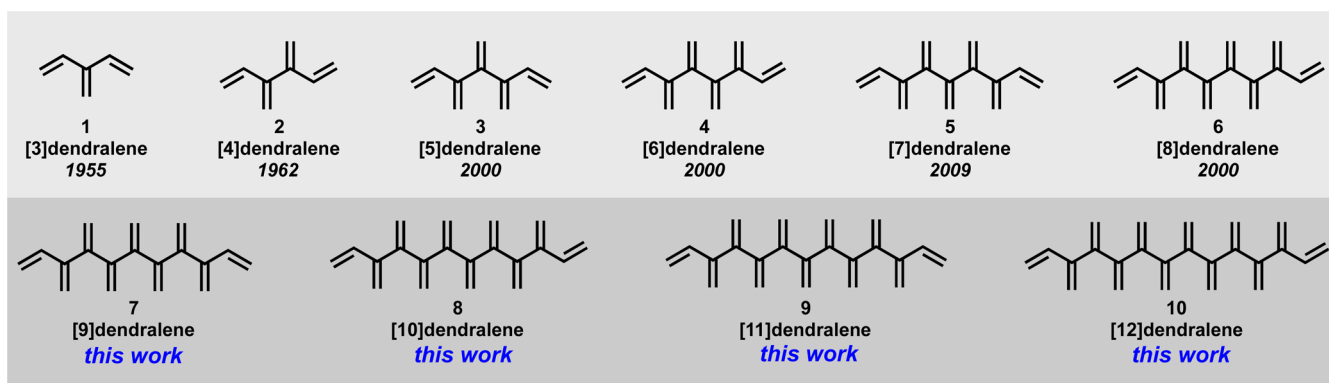


Figure 2. First ten members of the $[n]$ dendralene family of cross conjugated hydrocarbons and the year first reported.

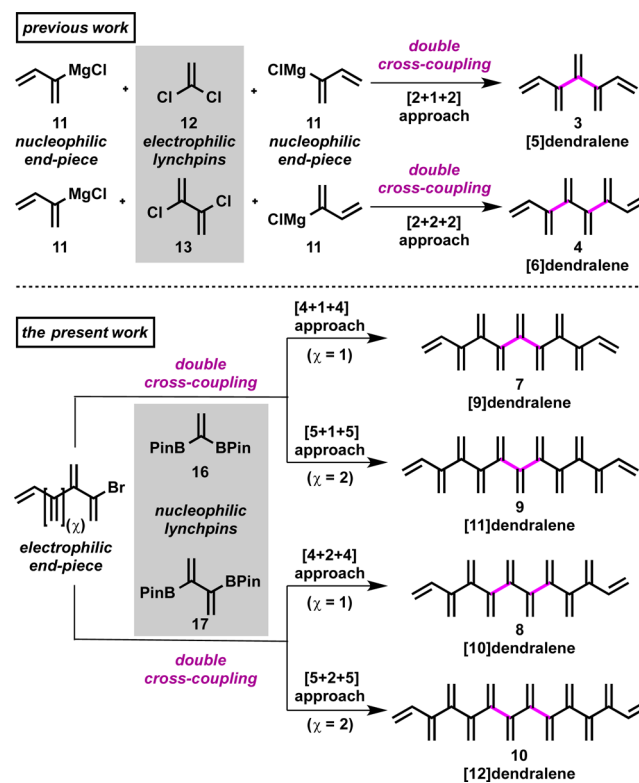
dienophile *N*-methylmaleimide (NMM), whereas, in contrast, the even parity dendralenes were shown to undergo unselective Diels–Alder reactions. Herein we report the first syntheses of the “higher” dendralenes, [9]–[12]dendralene (Figure 2). We also disclose a thorough investigation into the spectroscopic behavior and chemical reactivity of the first ten dendralenes ([3]–[12]dendralene inclusive), which unequivocally establish a diminishing, parity-dependent alternation in this fundamental hydrocarbon family.

RESULTS AND DISCUSSION

Synthesis. The early syntheses of [3]dendralene and [4]dendralene (Figure 2) involved classical pyrolytic elimination reactions of tri- and tetra-acyloxy (di-, tri-, and tetra-) derivatives of branched saturated hydrocarbons.^{5,9} No member of the family higher than the tetra-ene was reported prior to our contributions in this area. Due to the prevailing attitude at the time, specifically, that these compounds were likely to be unstable, our first synthesis of the family of $[n]$ dendralenes ($n = 3, 4, 5, 6$, and 8) involved first the preparation of 3-sulfolene derivatives of the hydrocarbons.⁷ The dendralenes were conveniently generated, a few mg at a time, by cheletropic elimination of SO_2 from these stable precursors. Our most recent contribution in this area involved the preparation of the complete family of the six “lowest” $[n]$ dendralenes ($n = 3, 4, 5, 6, 7$, and 8) by direct cross-couplings.⁸ The first three members of the family were prepared by one-step synthesis from commercially available precursors, whereas the synthesis of [6]-, [7]-, and [8]dendralene (4–6) mandates multistep syntheses.⁸ Until now, none of the “higher” dendralenes ([9]–[12]dendralene) (7–10) have been reported, most likely due to the significant synthetic challenge that these structures represent, along with the lack of availability of suitable coupling partners. A synthetic plan for the higher $[n]$ dendralenes, which draws upon the most synthetically powerful feature of our previous [5]- and [6]dendralene (3–4) synthesis, is depicted in Scheme 1. We propose that higher $[n]$ dendralenes are best prepared by employing a 2-fold cross-coupling process, between a bifunctional central unit (the “lynchpin”) and two identical monofunctional end-pieces. To prepare odd parity $[n]$ dendralenes, the lynchpin should contain an odd number of $\text{C}=\text{C}$ units; an even number of $\text{C}=\text{C}$ bonds in the lynchpin will furnish even $[n]$ dendralenes.²²

Our earlier approaches to [5]- and [6]dendralene (3–4) took advantage of this strategy, employing 2-fold cross-couplings between the chloroprene Grignard reagent (11), as a monofunctional nucleophilic end-piece, and the readily

Scheme 1. Proposal for a Lynchpin-Based, Double Cross-Coupling Approach to the $[n]$ Dendralenes



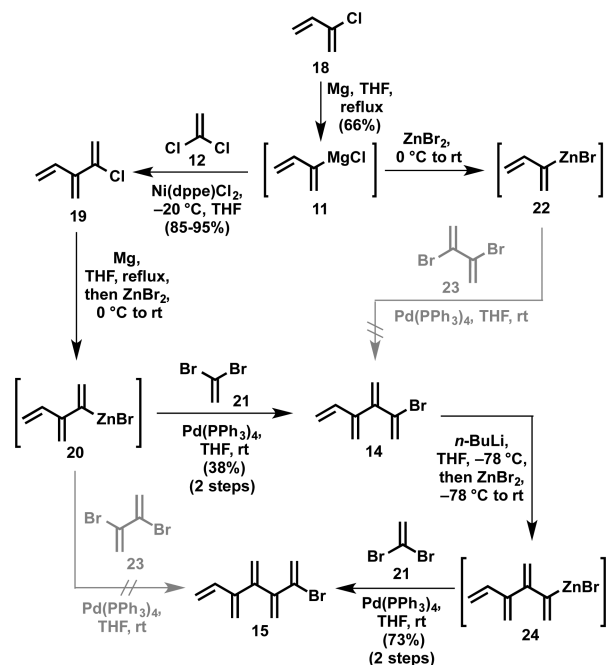
accessible lynchpin double electrophiles, 1,1-dichloroethylene (12) and 2,3-dichloro-1,3-butadiene (13), respectively (Scheme 1).⁸ [6]Dendralene (4) represents the limit of this approach for 1,3-butadiene coupling partners: either a dendralenic lynchpin or dendralenic end-piece are needed to prepare [7]dendralene (5) and higher.

Ultimately, we elected to pursue an approach involving the union of [4]- and [5]dendralenic end-pieces with the known ethylenic and 1,3-butadiene lynchpins. Both double electrophilic lynchpins^{23,24} and double nucleophilic lynchpins^{25,26} were already known, and their success in double cross-coupling reactions were proven.^{7,8,26–29} The synthetic problem was thus reduced to (a) the preparation of the dendralenic end-pieces, namely 2-halo[4]dendralene and 2-halo[5]dendralene, and (b) the successful deployment of these partners in double cross-coupling reactions.

The highest 2-halo[*n*]dendralene reported thus far is 2-chloro[4]dendralene.⁸ Frustratingly, this compound is unreactive as an electrophilic coupling partner in Kumada–Tamao–Corriu and Negishi cross-coupling reactions.⁸ In the hope of higher reactivity, we therefore targeted 2-bromo[4]dendralene (14) and its higher “ethenologue”, 2-bromo[5]dendralene (15).

In order to prepare 2-bromo[4]dendralene (14) and 2-bromo[5]dendralene (15) we envisioned a single sp^2 – sp^2 cross-coupling involving the 1,1-dibromoethylene (21)²³ and 2,3-dibromo-1,3-butadiene (23) lynchpins. During the course of these investigations it became evident that, whereas 1,1-dibromoethylene (21) participated in single cross-coupling reactions, 2,3-dibromo-1,3-butadiene (23) did not (Scheme 2).

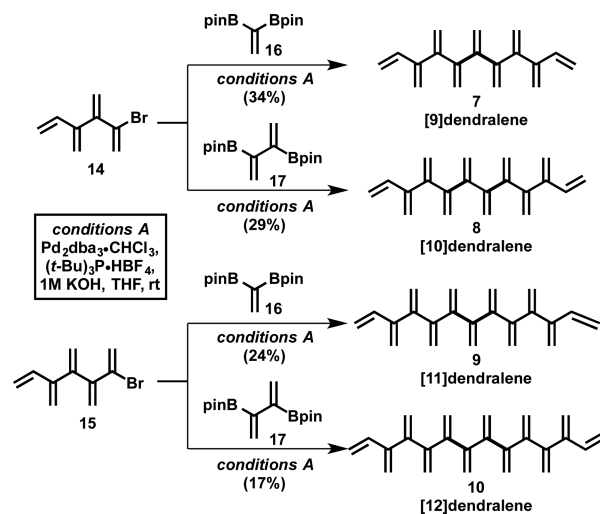
Scheme 2. Iterative Syntheses of 2-Bromo[4]dendralene (14) and 2-Bromo[5]dendralene (15)



(We presume that the product of oxidative insertion of L_n Pd(0) into the C–Br bond undergoes facile elimination of L_n Pd(II)–Br₂. Our suspicions are fuelled by the lack of reports of successful cross-coupling reactions involving 2,3-dibromo-1,3-butadiene (23) in the literature.) Thus, an iterative Negishi cross-coupling sequence with 1,1-dibromoethylene (21) was employed to convert the organozinc species derived from 2-chloro[3]dendralene (19)⁴ into 2-bromo[4]dendralene (14) (38% yield), and thence into 2-bromo[5]dendralene (15) (73% yield) (Scheme 2). The discrepancy in yield between these two steps is related to the method of preparation of the organozinc species: the latter case employed an efficient low temperature Li/Br exchange followed by transmetalation with ZnBr₂, whereas the former mandated the generation of the Grignard reagent in refluxing THF, which led to significant decomposition.

With the requisite end-pieces in hand, the synthesis of the higher dendralenes could now be attempted. Many different sets of conditions³⁰ were screened for the final 2-fold cross-coupling sequence, in which attempts were made to unite nucleophilic and electrophilic end-pieces with electrophilic and nucleophilic lynchpins, respectively (Scheme 3). Double cross-

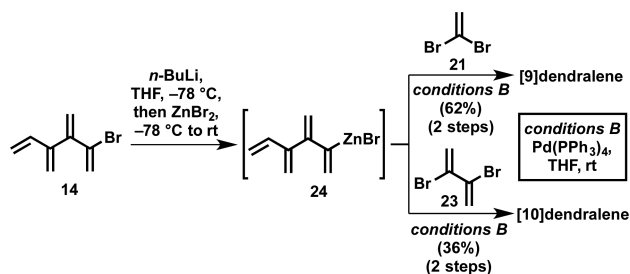
Scheme 3. Syntheses of [9]–[12]Dendralenes



coupling reactions between electrophilic lynchpins and nucleophilic end-groups were found to be particularly challenging transformations.³¹ Problematic side reactions include lynchpin eliminations³¹ and difficulties encountered in the generation of the nucleophilic component. Gratifyingly, the two nucleophilic lynchpins introduced by Hiyama and Shimizu^{25,26} successfully participated in Suzuki–Miyaura reactions, performed under Fu conditions, to deliver the desired higher dendralene in all four cases (Scheme 3).

[9]Dendralene (7) was synthesized in higher yield through a 2-fold Negishi cross-coupling reaction between the organozinc species 24 derived from 2-bromo[4]dendralene (14) and 1,1-dibromoethylene (21) (Scheme 4). [10]Dendralene (8) was

Scheme 4. Second Generation Syntheses of [9]- and [10]Dendralenes



also prepared through Negishi cross-coupling, in comparable yield to the Suzuki–Miyaura method. Interestingly, this protocol was not successful for the preparation of [11]- and [12]dendralene (9–10), with difficulties being encountered during the generation of the organometallic derivative of 2-bromo[5]dendralene.

Spectroscopic Studies. As mentioned earlier, one of the most striking features of our previous investigations into the dendralene family was the first observation of their parity-dependent alternation in behavior, which was manifested in (a) their UV–visible spectra; (b) their reactivity toward the dienophile *N*-methylmaleimide (NMM), and (c) their stability. With the present study giving access to an extended series of compounds, namely the first ten [*n*]dendralenes (1–10), we were keen to find out if parity-dependent behavior would be seen throughout the family.

The increasing conjugation witnessed in the parent all-*E*-linear polyenes (Figure 1) with increased chain length is evidenced by longer wavelengths (λ_{\max} increases by ca. 25 nm for each additional $-\text{HC}=\text{CH}-$ unit) and increasing molar extinction coefficients for their UV–visible absorption maxima.³² In contrast (Figure 3 (a)), the collection of nine

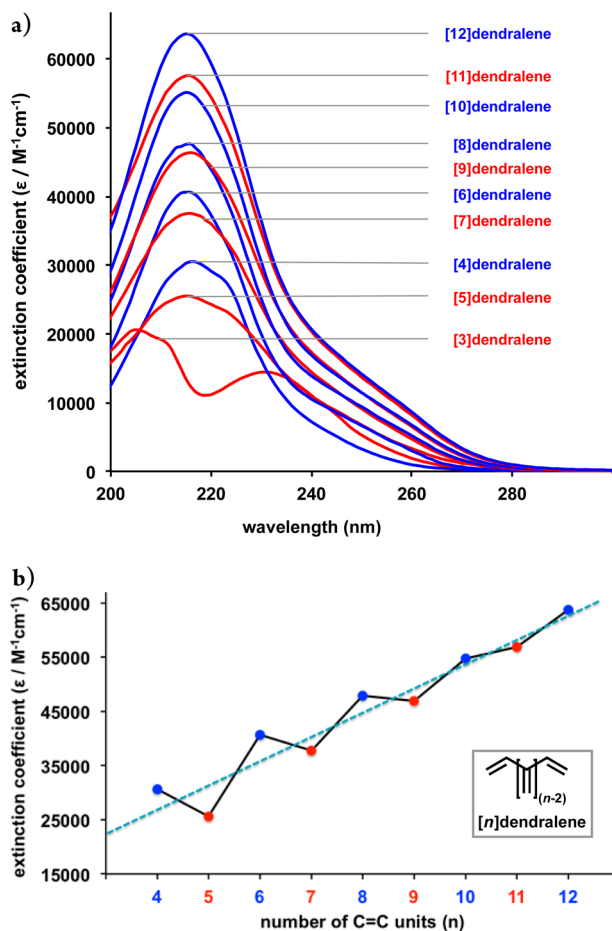


Figure 3. (a) UV–visible spectra of the [n]dendralene family, and (b) UV extinction coefficients (ϵ) of absorption maxima plotted as a function of the number of C=C bonds. $\lambda_{\max} = 215\text{--}216$ nm in all cases except [3]dendralene, which exhibits two maxima at 205 and 231 nm (hexane, 25 °C).

compounds [4]dendralene to [12]dendralene (2–10) show a single UV–visible absorption maximum at $\lambda_{\max} = 215\text{--}216$ nm (hexane), very close to that of 1,3-butadiene (217 nm, hexane).³³ The wavelength of the absorption exhibited by the dendralenes clearly shows that conjugation in these structures is restricted to 1,3-butadiene.

When the molar extinction coefficients are plotted against the number of C=C bonds present in the structure, a clear pattern of diminishing alternation emerges (Figure 3 (b)). Intriguingly, the inclusion of more C=C units does not give rise to gradually increasing extinction coefficient and instead, an alternating up–down pattern is seen for even and odd parity family members and notably, one whose magnitude decreases with increasing chain length. Within each of the two subfamilies of even and odd parity dendralenes, the incorporation of two C=C units (and hence progression to the next subfamily member) always results in an increase in extinction coefficient, and one of generally diminishing magnitude with progression

to higher family members.³⁴ Thus, the difference between extinction coefficients of the $\lambda_{\max} = 215\text{--}216$ nm absorption for [5]- and [6]dendralene (3–4) is relatively large ($\Delta\epsilon = 15100$), whereas the difference is relatively small ($\Delta\epsilon = 6000$) between [11]- and [12]dendralene (9–10). By extrapolating these experimental observations, at a rough approximation, the limit of measurable (by UV–visible spectroscopy) alternation should occur at [13]- or [14]dendralene and we predict a gradually increasing extinction coefficient for consecutive members of the dendralene family beyond this point.

To summarize the new findings from the UV–visible spectra of the dendralene family in the present study: first, all [n]dendralenes higher than the triene show a single absorption maximum at around the same wavelength as 1,3-butadiene. More accurate molar extinction coefficient values for [5]-dendralene (3) and [7]dendralene (5) have been obtained,³⁴ along with values for the previously unprepared [9]–[12]-dendralenes (7–10). These data confirm that the even parity dendralenes exhibit gradually increasing molar extinction coefficients and that this property extends to the higher members of the family. Importantly—and new to the present study—the odd dendralenes have also been shown to exhibit gradually increasing molar extinction coefficients with increasing chain lengths. When viewed together, the magnitudes of the UV–visible absorption maxima for the dendralene family exhibit an even/odd zigzag alternation, with a diminishing difference upon progression to higher members of the series (Figure 3b).

We initially assumed that the difference in behavior between even and odd parity dendralenes would be manifested only in UV–visible spectra. This assumption proved to be false: the diminishing alternation pattern is clearly visible in ^1H and ^{13}C NMR spectra of the dendralene family. ^1H NMR spectra of the first 11 members of the [n]dendralene family in CDCl_3 at 800 MHz are reproduced in Figure 4.

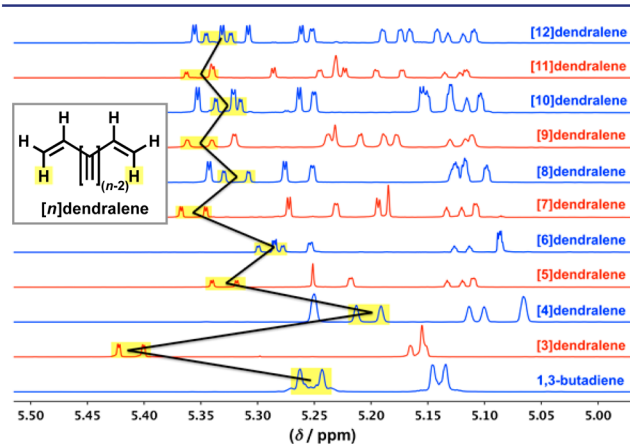


Figure 4. ^1H NMR spectra of the [n]dendralene family, exhibiting diminishing alternation in chemical shift of the Z-C1H resonance (800 MHz, CDCl_3 , 25 °C).

The diminishing alternation is observable in all three proton resonances associated with the terminal monosubstituted olefin on the branched chain, but it is most pronounced in the resonance of the proton residing on the terminal carbon cis- to the longest carbon chain (Z-C1H; δ 5.20–5.41 ppm: this resonance is highlighted in yellow in Figure 4). Thus, the Z-C1H chemical shift difference is largest ($\Delta\delta = 0.21$ ppm) between [3]dendralene (1) (δ 5.41 ppm) and [4]dendralene

(2) (δ 5.20 ppm), and smallest ($\Delta\delta = 0.02$ ppm) between [11]dendralene (9) (δ 5.35 ppm) and [12]dendralene (10) (δ 5.33 ppm), with the variance diminishing with progression up the series.

^{13}C NMR spectra of the first 11 members of the [n]dendralene family in CDCl_3 at 200 MHz are reproduced

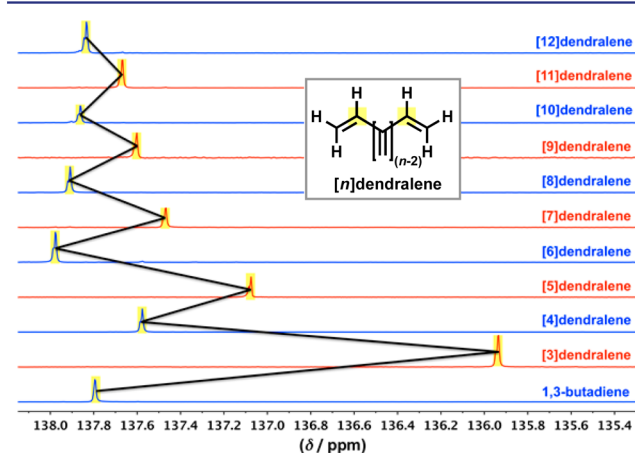


Figure 5. ^{13}C NMR spectra of the [n]dendralene family, exhibiting diminishing alternation in chemical shift of the C2 methine resonance (200 MHz, CDCl_3 , 25 °C).

in Figure 5. The diminishing alternation is observable in both ^{13}C resonances associated with the terminal monosubstituted olefin of the branched chain, but it is most pronounced in the C2 methine resonance (δ 138.0–135.9 ppm: this resonance is highlighted in yellow in Figure 5). Again, the chemical shift difference is largest ($\Delta\delta = 1.7$ ppm) between [3]dendralene (1) (δ 135.9 ppm) and [4]dendralene (2) (δ 137.6 ppm) and smallest ($\Delta\delta = 0.1$ ppm) between [11]dendralene (9) (δ 137.7 ppm) and [12]dendralene (10) (δ 137.8 ppm), with the variance diminishing with progression up the series.

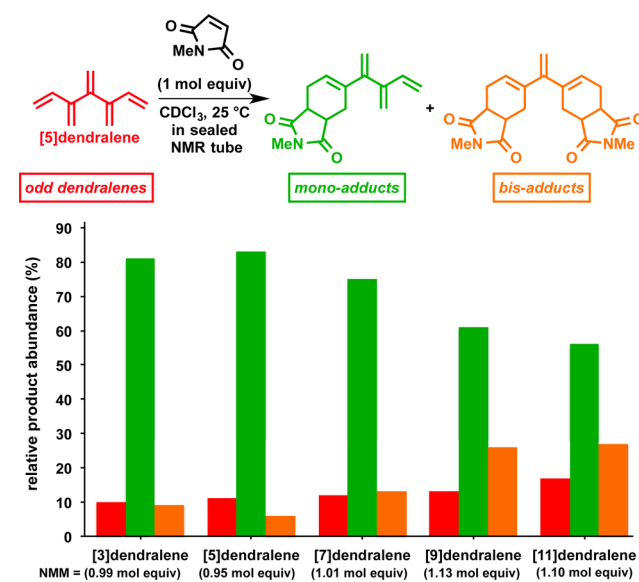
Diels–Alder Reactions. In our earlier investigation⁸ on [3]–[8]dendralenes (1–6), it was demonstrated that parity-dependent behavior was also manifested in the chemical reactivity of the hydrocarbons. Whereas all dendralenes were shown to react as dienes in Diels–Alder cycloadditions with the electron-poor dienophile *N*-methylmaleimide (NMM) regioselectively at the terminal 1,3-butadiene residue, odd and even parity dendralenes reacted differently. Specifically, when exposed to 1 mol equiv of the dienophile, odd parity dendralenes underwent predominantly single cycloaddition, whereas even dendralenes gave mixtures of single and double adducts along with unreacted dendralene. It was also observed experimentally that odd parity dendralenes were significantly more reactive than even parity ones. Single cycloaddition occurs with odd parity dendralenes because the product of monoaddition to the terminal diene site with a dienophile generates an even dendralene, which is less reactive than the precursor but the converse is true for the even parity hydrocarbons. Would this divergent reactivity for even and odd systems hold for all dendralenes? With the higher dendralenes in hand, we set about answering this question and, at the same time, we re-examined the outcomes of reactions of the lower dendralenes to a higher level of precision.

The Diels–Alder reactions of [3]- to [12]dendralenes (1–10) toward the dienophile NMM (1.00 \pm 0.10 mol equiv) were

examined in ca. 0.3 M CDCl_3 solutions at 25 °C, with the progress of reactions being followed, and the product compositions being analyzed by 800 MHz ^1H NMR spectroscopy. Isolated yields were consistent with crude product compositions. All reactions were run until all NMM was consumed and in every case, mixtures of unreacted starting materials, monocycloadducts and bis-cycloadducts were generated. With the exception of [4]dendralene (2), the majority of the monoadduct fraction was the product of addition to the terminal 1,3-butadiene unit of the dendralene, and the major bis-cycloadducts were those resulting from additions to the two ends of the dendralene chain.³⁵

The outcomes of reactions of the odd parity dendralenes are depicted in Chart 1. All reactions produce the monoadduct as

Chart 1. Diels–Alder Reactions of Odd Dendralenes (Diene) with 1 mol Equiv of NMM (Dienophile)



the major product. As the odd parity dendralene subfamily is ascended, the selectivity for monoaddition generally deteriorates, and the amounts of unreacted starting dendralene and bis-adducts increases.

The outcomes of reactions of the even parity dendralenes with NMM are depicted in Chart 2. All reactions are less selective than those of the odd parity dendralenes. Nonetheless, as the even parity dendralene subfamily is ascended, there is a gradual improvement in the selectivity for the monoaddition product, with amounts of unreacted starting dendralene and bis-adducts decreasing.

When the selectivity for the monoadduct is graphed for the complete dendralene family, the diminishing alternation pattern is revealed once again (Chart 3). Thus, the gradually diminishing selectivity for the monoadduct in the odd parity subseries interweaves with the steadily improving selectivity in the even dendralenes, with a significant difference between the lower family members but a negligible difference in selectivity for the highest members.

Computational studies were conducted to explain these experimental findings. Our investigations commenced with a detailed analysis of the conformational preferences of the dendralenes.

Computational Studies. Conformational Analysis. The conformations and energies of the series of [n]dendralenes ($n =$

Chart 2. Diels–Alder Reactions of *Even* Dendralenes (Diene) with 1 mol Equiv of NMM (Dienophile)

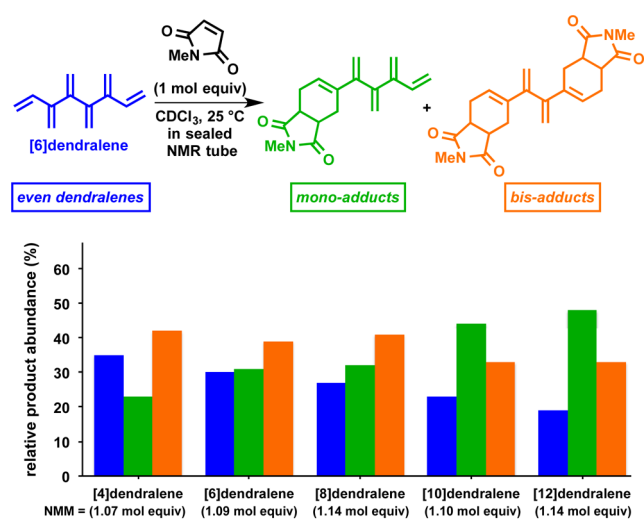
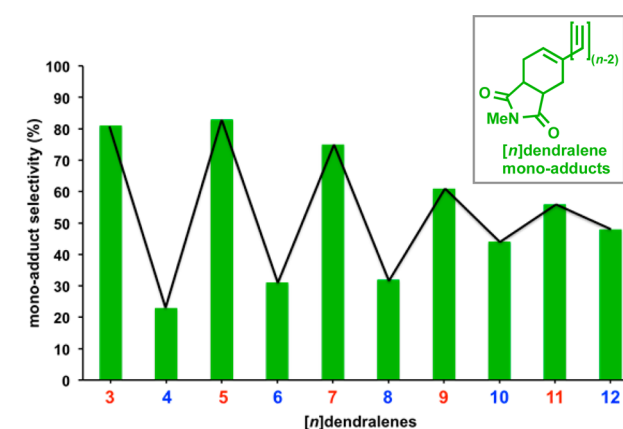


Chart 3. Selectivity for Mono-Cycloaddition in Diels–Alder Reactions of $[n]$ Dendralenes (Diene) with 1 mol Equiv of NMM (Dienophile)



3–8) were obtained using the accurate composite ab initio MO G4(MP2) procedure.³⁶ We first confirmed the suitability of G4(MP2) to handle the task in hand by applying it to the conformational analysis of 1,3-butadiene. We calculated the rotational barrier to the conversion of the more stable C_{2h} anti conformer to the C_2 gauche conformer to be $\Delta H^\ddagger(0\text{ K}) = 23.9$ kJ/mol and the gauche–anti energy difference to be $\Delta H^\ddagger(0\text{ K}) = 12.4$ kJ/mol, favoring the anti conformer and these energies are in satisfactory agreement with the experimental³⁷ values of $\Delta H^\ddagger(0\text{ K}) = 24.8$ kJ/mol and $\Delta H^\ddagger(0\text{ K}) = 11.9$ kJ/mol, respectively.

The structures of [3]dendralene and [4]dendralene have been determined using gas phase electron diffraction^{11,38} and their conformations have been studied computationally using a variety of methods.^{11,38,39} Our G4(MP2) calculations on these two dendralenes are in general agreement with these earlier studies. [3]Dendralene has three stable conformations and they are shown in Figure 6, together with the transition structures for their interconversion and relative energies. The most stable conformation is anti-gauche, in which the two dihedral angles between the double bonds in the anti and gauche units are 174° and 41° , respectively. The gauche dihedral angle is 11° larger than that calculated for 1,3-butadiene, which probably reflects the presence of steric repulsion between the terminal vinyl groups in the anti–gauche conformer. The anti–anti conformer is only 3.7 kJ/mol above the anti–gauche structure and has C_2 symmetry. The anti-butadiene units are rather bent, the dihedral angle between the vinyl groups in each unit being 157° . This bending is probably due to steric congestion between the Z-C1H atoms of the terminal methylene groups, their separation being 2.22 Å. The C_2 symmetric gauche–gauche conformer is the least stable, lying 9.8 kJ/mol above the anti–gauche conformer. The dihedral angle between adjacent vinyl groups is 33° . The anti–gauche/anti–anti/gauche–gauche distribution at 25 °C is calculated to be 82:16:2, respectively. The rotational barriers for the conversion of the anti–gauche conformer into the anti–anti and gauche–gauche conformers are 7.7 and 20.0 kJ/mol, respectively. These barriers, particularly the former, are sufficiently small enough to permit rapid conformer interconversion on the NMR time scale, as we have confirmed experimentally for the whole series of dendralenes studied herein (see above).

The most stable conformation of [4]dendralene was shown by gas phase electron diffraction to comprise two anti-butadiene groups twisted 72° with respect to each other.¹¹ MP2/6-311G(d) calculations located five conformations of this molecule, the most stable being identical to that found experimentally.¹¹ The G4(MP2) calculations gave similar results and the two lowest energy conformations, of the five that were located, are shown in Figure 7. The most stable conformation has C_2 symmetry with the two anti-1,3-butadiene units making a 76° dihedral angle with respect to the two internal double bonds. The dihedral angle between the double bonds within each anti-butadiene group is 174° . The next most stable conformer is 10.3 kJ/mol higher in energy (Figure 7) than the global minimum energy conformer and consists of an anti-butadiene attached to a gauche-butadiene moiety in which the twist angle is 30° . The dihedral angle between the two internal double bonds in this conformer is 54° . A gaseous sample of [4]dendralene at 25 °C is calculated to contain ca. 97% of the bis-anti-butadiene conformer (cf. ca. 90% from MP2 calculations¹¹).

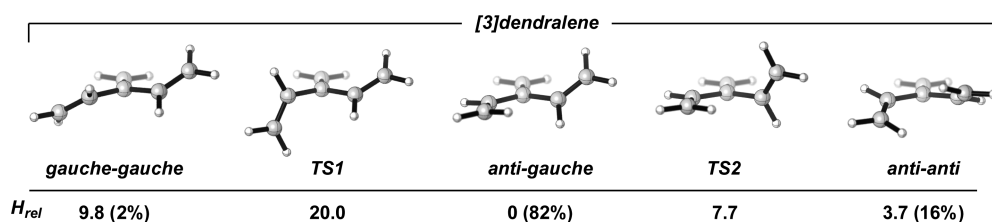


Figure 6. G4(MP2) optimized geometries of conformations and transition structures of [3]dendralene. H_{rel} (kJ/mol) refers to 0 K. Populations were derived from free energy data at 25 °C. Values in parentheses are the percentage population values.

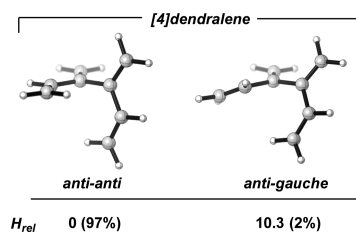


Figure 7. G4(MP2) optimized geometries of the two lowest energy conformations of [4]dendralene. H_{rel} (kJ/mol) refers to 0 K and percentage populations are for 25 °C (the residual 1% is spread over the remaining three higher energy conformations). Values in parentheses are the percentage population values.

These findings lead to a generalization concerning the preferred conformation of dendralenes, particularly those containing even numbers of double bonds, namely that it possesses the maximum possible number of *anti*-butadiene units. This prediction was confirmed for [6]dendralene and [8]dendralene; of the 16 and ten conformations located for the former and latter dendralene, respectively, the most stable conformer for each dendralene does possess the maximal *anti*-butadiene count (Figure 8). In fact, we found two such

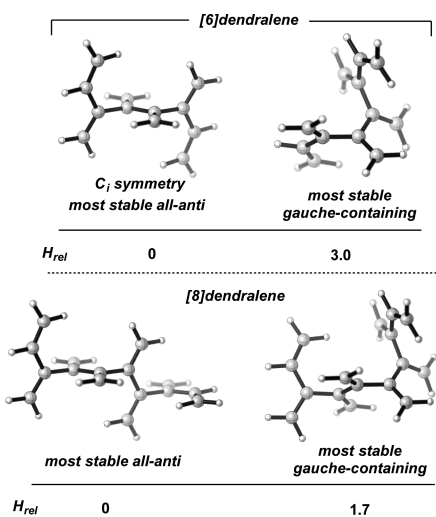


Figure 8. G4(MP2) optimized geometries of the global minimum energy structures (left) and lowest energy structures possessing a *gauche* butadiene unit (right) for [6]dendralene and [8]dendralene; H_{rel} (0 K) in kJ/mol.

conformers of [6]dendralene which possessed three *anti*-butadiene moieties, one of C_i symmetry (Figure 8) and the other of C_2 symmetry (not shown). Similarly, there are three conformers of [8]dendralene which possess four *anti*-butadiene groups, two of C_2 symmetry and the other of C_1 symmetry. The most stable conformers of [6]dendralene and [8]dendralene, each of which possesses a single *gauche*-butadiene conformation within its structure, are also shown in Figure 8. In both conformers, the *gauche*-butadiene group is sandwiched between *anti*-butadienes. The energy difference between the all-*anti*-butadiene conformer and the most stable conformer with a *gauche*-butadiene unit decreases along the series [4]dendralene > [6]dendralene > [8]dendralene, that is 10.3, 3.0, and 1.7 kJ/mol, respectively. Consequently, this trend, together with the increase in the number of different *gauche* conformers with increasing dendralene chain length, the population of the all-

anti-butadiene conformers decreases rapidly with increasing chain length. The number of different lowest energy conformers of the even-membered series of [n]dendralenes ($n = 4, 6, 8$) which lie within 3 kJ/mol of each other, and whose combined abundances add up to more than 80% of the mixture at 25 °C, increases along the series, from one ($n = 4$), to three ($n = 6$), to five ($n = 8$).

The two lowest energy conformers of the odd-membered [5]dendralene and [7]dendralene may be described as the attachment of *anti*-butadiene groups to either an *anti-anti*- or *anti-gauche*-[3]dendralene unit (Figure 9), although this

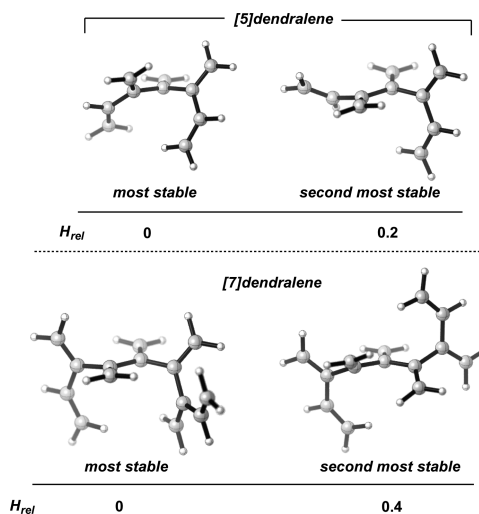


Figure 9. G4(MP2) optimized geometries of the two lowest energy conformers of [5]dendralene and [7]dendralene; H_{rel} (0 K) in kJ/mol.

characterization becomes less definite in the case of [7]-dendralene. The terminal double bonds in these dendralenes may adopt either a *gauche* or an *anti* orientation with respect to its adjacent double bond. The percentage of those conformations bearing at least one terminal *gauche* vinyl group decreases with increasing chain length in the odd-membered series of [n]dendralenes.

Computed NMR Chemical Shifts. Using the method of Tantillo et al.,⁴⁰ the ^1H and ^{13}C chemical shifts (in chloroform) for the terminal methylene *Z*-C1H proton and C2 methine carbon, respectively, were calculated for various conformers of the series of [n]dendralenes, for $n = 3$ –8. The chemical shifts for the three conformations of [3]dendralene and the major conformer of [4]dendralene are depicted in Figure 10.

Upon changing the conformation of the terminal butadienyl group from *gauche* to *anti*, the methylene *Z*-C1H and C2

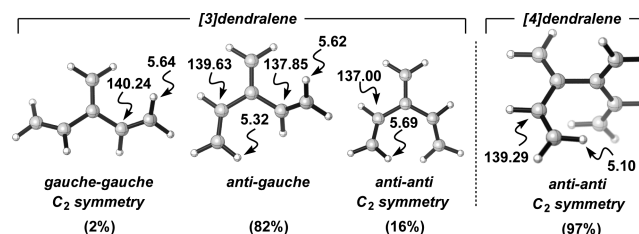


Figure 10. Calculated ^1H and ^{13}C chemical shifts (δ /ppm, in chloroform) for the terminal methylene *Z*-C1H proton and C2 methine carbon; percentage abundances at 25 °C. Values in parentheses are the percentage population values.

methine ^{13}C nuclei experience upfield and downfield shifts of ca. 0.5 and 1.5 ppm, respectively (cf. *anti-gauche*-[3]-dendralene with [4]dendralene). Since the even-membered dendralenes favor all-*anti*-butadiene units and the odd-membered series are populated with *gauche*-butadiene groups, the average chemical shifts of the aforementioned nuclei should display oscillatory behavior with increasing dendralene length, although it should be progressively damped as the even- and odd-membered dendralenes acquire increasing populations of, respectively, terminal *gauche*- and *anti*-butadiene groups with increasing dendralene length. This damped oscillatory behavior is observed both experimentally and computationally (Figures 4 and 5, Table 1). The computational values in Table 1 were

Table 1. Calculated weighted average chemical shifts for the terminal methylene Z-C1H and C2 methine ^{13}C nuclei of [*n*]dendralenes

dendralene	^1H	^{13}C
[3]dendralene	5.51	138.74
[4]dendralene	5.10	139.29
[5]dendralene	5.37	138.84
[6]dendralene	5.27	139.19
[7]dendralene	5.38	139.21
[8]dendralene	5.29	139.53

derived from calculating the average of the chemical shifts of interest associated with both terminal vinyl groups of each conformer and then taking the conformer-weighted average of these chemical shifts. The qualitative agreement between experimental and calculated trends in chemical shifts along the dendralene series is acceptable and confirms the origin of the oscillatory behavior to conformational effects rather than to parity-dependent electronic effects.

Calculations of Excited States. Time-dependent (TD) theory, using the ωB97X functional,⁴¹ was employed to calculate the lowest energy (π , p^*) transitions in selected dendralenes and the results for all conformations of [3]-dendralene and for the major conformer of [4]dendralene, which dominates the equilibrium mixture of conformers (97%), are presented in Table 2.

The calculated electronic transitions corresponding to 235 and 202 nm for the major *anti-gauche* conformer of [3]dendralene (82%) are in reasonable agreement with the experimental λ_{max} values of 231 and 205 nm. The *anti-anti*

Table 2. TD- $\omega\text{B97X}/6-311+\text{G}(22\text{d},\text{p})^a$ Vertical Excitations, Expressed in Wavelengths (nm), and Experimental Values

molecule	conformer	calcd. λ [<i>f</i>] ^b	exptl. λ_{max} ^c
[3]dendralene	<i>anti-gauche</i>	235 [0.41]	231
		202 [0.53]	205
	<i>anti-anti</i>	235 [0.64]	
		212 [0.15]	
		246 [0.12]	
<i>gauche-gauche</i>	206 [0.58]		
	224 [0.31]	216	
[4]dendralene	<i>bis-anti</i>	222 [0.40]	
		213 [0.21]	
		212 [0.37]	

^aHeptane solvent using the PCM method. ^bOscillator strength. ^cValues for equilibrium mixture of conformers.

conformer of [3]dendralene, which makes up 16% of the equilibrium mixture of conformers at 25 °C, is predicted to have excitation energies very similar to those of the *anti-gauche* conformer, although the shorter wavelength transition exhibits a 10 nm bathochromic shift, relative to the latter conformer. The longer wavelength transition in the *gauche-gauche* conformer displays a 11 nm bathochromic shift, relative to the other two conformers, but this has no importance to the current investigation owing to its negligible 2% abundance in the mixture. The two lowest electronic transitions of each conformer of [3]dendralene are well-separated in energy and they give rise to distinct Franck–Condon bands, as we have observed experimentally (Figure 3a). This distinct separation between the bands probably reflects the fairly strong degree of conjugative coupling between adjacent double bonds. For example, the 41° dihedral angle between the two double bonds in the *gauche*-butadienyl group in the major *anti-gauche* conformer suggests a coupling strength within this group that is about 50% of that within the *anti*-butadienyl group.

The situation becomes more complex for the higher members of the [*n*]dendralenes. Our TD calculations on the predominant conformer of [4]dendralene predict four transitions lying within the range 212–224 nm and all having oscillator strengths greater than 0.2. This tight bunching of the excitation wavelengths may be attributed to the large value of the dihedral angle of 76° between the adjacent double bonds from the two *anti*-butadienyl groups, a value which implies a coupling strength between the two *anti*-butadienyl groups of only ca. 6% of that between two double bonds within the *anti*-butadienyl group. Thus, these four close lying transitions, once Franck–Condon factors and solvent effects are taken into account, may well give rise to a broad featureless absorption band that is observed experimentally. As the dendralene chain length increases, the number of electronic transitions per conformer increases, as does the number of conformers in the dendralene mixture. For example, our TD calculations on [8]dendralene predict a total number of 39 transitions lying within 206–237 nm for the four conformers which constitute ca. 80% of the mixture. The most intense transitions occur in the 210–220 nm range, which is consistent with the experimental observation that the maximum absorption occurs at 216 nm and that the band is very broad.

In summary, our TD calculations on [*n*]dendralenes qualitatively reproduce the main features of the experimentally observed UV–visible absorption spectra of the dendralenes, namely that the relatively strong electronic coupling between adjacent double bonds in [3]dendralene leads to two distinct absorption bands, whereas weaker coupling between contiguous *anti*-butadienyl groups in the higher homologues produces broad featureless bands for $n > 3$.

Diels–Alder Reactions. Experimentally, [3]dendralene was found to be substantially more reactive than [4]dendralene toward Diels–Alder dimerization and its Diels–Alder reaction with *N*-methylmaleimide (NMM). G4(MP2) calculations on these reactions traced the origin of this reactivity difference to the difference in populations of the reactive conformation in the two dendralenes.⁴² The major conformer of [3]dendralene possesses a *gauche* butadiene moiety which is predisposed to participate in a Diels–Alder reaction. In contrast, the major conformer of [4]dendralene (97%) possesses two *anti*-butadienyl groups; consequently, a distortion energy penalty must be paid by [4]dendralene to convert an *anti*-butadiene group into its reactive *gauche* conformation. We may generalize

this argument to state that the Diels–Alder reactivity of $[n]$ dendralenes is parity-dependent. That is, those dendralenes with odd values of n (which necessarily possess at least one *gauche*-butadienyl group) should be more reactive than their neighbors with even values of n .

This generalization was tested by calculating the six lowest energy endo transition states (TSs) for the NMM Diels–Alder additions to $[5]$ dendralene and $[6]$ dendralene. The G4(MP2) activation energy for the lowest energy pathway for each of these reactions are given in Table 3, together with those reported⁴² for $[3]$ dendralene and $[4]$ dendralene.

Table 3. G4(MP2) Activation Enthalpies and Free Energies for the Diels–Alder Reaction between *N*-Methylmaleimide (NMM) and $[n]$ Dendralenes

dendralene	ΔH^\ddagger (0 K) ^a	ΔG^\ddagger (298 K) ^a
$[3]$ dendralene	34.9 ^b	93.5 ^b
$[4]$ dendralene	46.6 ^b	105.0 ^b
$[5]$ dendralene	32.2	87.1
$[6]$ dendralene	41.9	104.2

^akJ/mol. ^bRef 42.

The data in Table 3 clearly reveal the parity-dependent, oscillatory behavior of the activation energies, those for odd parity dendralenes lying well below the even parity ones. The energy required to convert the most stable conformer of $[4]$ dendralene and $[6]$ dendralene is about 13 and 8 kJ/mol, respectively and is consistent with the aforementioned explanation of the origin of the parity effect.⁴²

Finally, we investigated, using G4(MP2) and B3LYP/6-31G(d) model chemistries, the regioselectivities of the Diels–Alder reactions of $[n]$ dendralenes for $n = 4–6$. Experimentally, *terminal* addition of NMM is preferred over *internal* addition. First, we investigated endo/exo selectivity in the Diels–Alder reactions involving $[4]$ dendralene and $[5]$ dendralene. It was found that endo addition was favored over exo addition by more than 12 kJ/mol. Consequently, attention was paid only to endo modes of addition. The lowest energy B3LYP/6-31G(d) TS for each site of addition of NMM to the dendralenes are shown in Figure 11, together with the B3LYP and G4(MP2) relative enthalpies (0 K).

These TSs show a relatively small degree of bond length asynchronicity, with the TSs for *internal* addition to $[5]$ - and $[6]$ dendralene displaying the largest values of $\Delta r = 0.32$ and 0.33 Å, respectively. Whereas B3LYP correctly predicts *terminal* selectivity for all three dendralenes, the G4(MP2) method incorrectly predicts preferred *internal* addition by NMM on $[4]$ dendralene. Moreover, the B3LYP method predicts much stronger *terminal* preferences than does G4(MP2), which is more in keeping with the strong preference observed experimentally. Thus, on the basis of the free energies of all TS conformations for each position of addition at 25 °C, the *terminal/internal* ratio is only 60:40 for G4(MP2), but 86:14 for B3LYP. The ratios are comparable for $[6]$ dendralene, being 86:14 (G4(MP2)) and 94:6 (B3LYP).

The preferred *terminal* site selection by NMM may be understood in terms of steric interactions between spectator groups at positions 2 and 3 of the reactive butadiene component of the dendralene. In the *terminal* mode of addition, only position 2 bears a non-hydrogen substituent, whereas both 2 and 3 positions are substituted when *internal* addition takes place. The steric argument is also consistent with

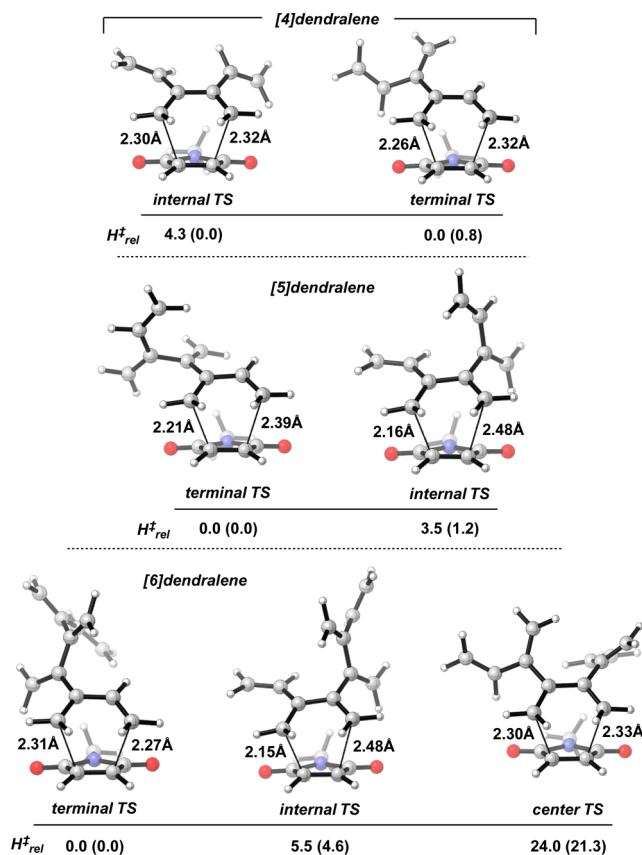


Figure 11. B3LYP/6-31G(d) lowest energy endo transition structures (TSs) for the different modes of addition of *N*-methylmaleimide (NMM) to $[4]$ -, $[5]$ - and $[6]$ dendralenes. H^\ddagger_{rel} (0 K) in kJ/mol. Values in parentheses are the G4(MP2) values.

the prediction that, of the two different modes of *internal* addition by NMM on $[6]$ dendralene, addition to the central diene moiety, which bears two 2'-butadienyl groups at positions 2 and 3, is strongly disfavored, compared to addition at the other *internal* diene, which has a vinyl and 2'- $[3]$ dendralenyl substituents at positions 2 and 3.

CONCLUSIONS

The simplest cross-conjugated triene, $[3]$ dendralene, and cross-conjugated tetraene, $[4]$ dendralene, exhibit very different physical and chemical behaviors. This odd versus even parity difference continues through the family but gradually fades with increasing numbers of C=C units until the difference becomes negligible in compounds with more than ten C=C bonds. This dampening oscillation has been recorded experimentally in extinction coefficients of UV–visible spectra, and in chemical shifts in both ¹H and ¹³C NMR spectra. The same effect has also been measured experimentally in the Diels–Alder reactions of the series of $[n]$ dendralenes with the dienophile *N*-methylmaleimide.

The diminishing alternation trend observed on ascending the family of $[n]$ dendralenes has been traced to conformational effects. The conformational preferences of the dendralenes contrast most strongly between $[3]$ dendralene and $[4]$ dendralene, the former exhibiting a preferred conformation with a *gauche*-butadiene moiety, with the latter displaying two *anti*-butadienes at an angle of 72° to one another. With increasing chain length, for odd $[n]$ dendralenes, the percentage

of conformations bearing at least one terminal *gauche* vinyl group decreases, whereas for even $[n]$ dendralenes, the percentage of conformations bearing at least one terminal *gauche* vinyl group increases. It is these conformational preferences which determine the physical and chemical properties of the branched acyclic polyenes.

■ ASSOCIATED CONTENT

Supporting Information

The Supporting Information is available free of charge on the ACS Publications website at DOI: 10.1021/jacs.5b11889.

Synthetic and computational work (PDF)

■ AUTHOR INFORMATION

Corresponding Authors

*m.paddonrow@unsw.edu.au

*michael.sherburn@anu.edu.au

Notes

The authors declare no competing financial interest.

■ ACKNOWLEDGMENTS

M.N.P.-R. acknowledges that this research was undertaken with the assistance of resources provided at the NCI National Facility through the National Computational Merit Allocation Scheme supported by the Australian Government. We thank Joshua Boyle, Nicholas Green, and Erik Lindeboom (ANU) for provision of [3]dendralene, [4]dendralene, and [6]dendralene, respectively. This work was supported by the Australian Research Council.

■ REFERENCES

- (1) (a) Hopf, H. *Angew. Chem., Int. Ed. Engl.* **1984**, *23*, 948. (b) Hopf, H.; Sherburn, M. S. *Angew. Chem., Int. Ed.* **2012**, *51*, 2298.
- (2) Sherburn, M. S. *Acc. Chem. Res.* **2015**, *48*, 1961.
- (3) Hopf, H. *Classics in Hydrocarbon Chemistry: Syntheses, Concepts, Perspectives*; Wiley-VCH: Weinheim, 2000; pp 103–309.
- (4) Bradford, T. A.; Payne, A. D.; Willis, A. C.; Paddon-Row, M. N.; Sherburn, M. S. *Org. Lett.* **2007**, *9*, 4861.
- (5) (a) Blomquist, A. T.; Verdol, J. A. *J. Am. Chem. Soc.* **1955**, *77*, 81. (b) Bailey, W. J.; Economy, J. *J. Am. Chem. Soc.* **1955**, *77*, 1133. (c) Trahanovsky, W. S.; Koepfinger, K. A. *J. Org. Chem.* **1992**, *57*, 4711.
- (6) (a) Blomquist, A. T.; Verdol, J. A. *J. Am. Chem. Soc.* **1955**, *77*, 1806. (b) Bailey, W. J.; Cunov, C. H.; Nicholas, L. *J. Am. Chem. Soc.* **1955**, *77*, 2787. (c) Martin, H.-D.; Eckert-Maksić, M.; Mayer, B. *Angew. Chem., Int. Ed. Engl.* **1980**, *19*, 807. (d) Priebe, H.; Hopf, H. *Angew. Chem., Int. Ed. Engl.* **1982**, *21*, 286. (e) Vdovin, V. M.; Finkel'shtein, E.; Sh; Shelkov, A. V.; Yatsenko, M. S. *Bull. Acad. Sci. USSR, Div. Chem. Sci.* **1986**, *35*, 2364. (f) Cadogan, J. I. G.; Cradock, S.; Gillam, S.; Gosney, I. *J. Chem. Soc., Chem. Commun.* **1991**, 114. (g) Bradford, T. A.; Payne, A. D.; Willis, A. C.; Paddon-Row, M. N.; Sherburn, M. S. *J. Org. Chem.* **2010**, *75*, 491. (h) Toombs-Ruane, H.; Osinski, N.; Fallon, T.; Wills, C.; Willis, A. C.; Paddon-Row, M. N.; Sherburn, M. S. *Chem. - Asian J.* **2011**, *6*, 3243.
- (7) Fielder, S.; Rowan, D. D.; Sherburn, M. S. *Angew. Chem., Int. Ed.* **2000**, *39*, 4331.
- (8) Payne, A. D.; Bojase, G.; Paddon-Row, M. N.; Sherburn, M. S. *Angew. Chem., Int. Ed.* **2009**, *48*, 4836.
- (9) Bailey, W. J.; Nielsen, N. A. *J. Org. Chem.* **1962**, *27*, 3088.
- (10) (a) Skattebøl, L.; Solomon, S. *J. Am. Chem. Soc.* **1965**, *87*, 4506. (b) Grimme, W.; Rother, H.-J. *Angew. Chem., Int. Ed. Engl.* **1973**, *12*, 505. (c) Bee, L. K.; Everett, J. W.; Garratt, P. J. *Tetrahedron* **1977**, *33*, 2143. (d) Roth, W. R.; Scholz, B. P.; Breuckmann, R.; Jelich, K.; Lennartz, H.-W. *Chem. Ber.* **1982**, *115*, 1934. (e) Payne, A. D.; Willis, A. C.; Sherburn, M. S. *J. Am. Chem. Soc.* **2005**, *127*, 12188.
- (11) Brain, P. T.; Smart, B. A.; Robertson, H. E.; Davis, M. J.; Rankin, D. W. H.; Henry, W. J.; Gosney, I. *J. Org. Chem.* **1997**, *62*, 2767.
- (12) (a) Hopf, H.; Maas, G. *Angew. Chem., Int. Ed. Engl.* **1992**, *31*, 931. (b) Maas, G.; Hopf, H. *Synthesis and Transformation of Radialenes [Online]*; PATAI's Chemistry of Functional Groups, John Wiley & Sons, Ltd.: New York, 2009; pp 1–51. (c) Hopf, H. *Classics in Hydrocarbon Chemistry: Syntheses, Concepts, Perspectives*; Wiley-VCH: Weinheim, 2000; pp 290–300.
- (13) (a) Dorko, E. A. *J. Am. Chem. Soc.* **1965**, *87*, 5518. (b) Waitkus, P. A.; Sanders, E. B.; Peterson, L. I.; Griffin, G. W. *J. Am. Chem. Soc.* **1967**, *89*, 6318. (c) Kozhushkov, S. I.; Leonov, A.; de Meijere, A. *Synthesis* **2003**, *2003*, 956. (d) Wright, C.; Holmes, J.; Nibler, J. W.; Hedberg, K.; White, J. D.; Hedberg, L.; Weber, A.; Blake, T. A. *J. Phys. Chem. A* **2013**, *117*, 4035.
- (14) Trabert, L.; Hopf, H. *Liebigs Ann. Chem.* **1980**, *1980*, 1786.
- (15) Mackay, E. G.; Newton, C. G.; Toombs-Ruane, H.; Lindeboom, E. J.; Fallon, T.; Willis, A. C.; Paddon-Row, M. N.; Sherburn, M. S. *J. Am. Chem. Soc.* **2015**, *137*, 14653–14659.
- (16) (a) Harruff, L. G.; Brown, M.; Boekelheide, V. *J. Am. Chem. Soc.* **1978**, *100*, 2893. (b) Höpfner, T.; Jones, P. G.; Ahrens, B.; Dix, I.; Ernst, L.; Hopf, H. *Eur. J. Org. Chem.* **2003**, *2003*, 2596.
- (17) (a) Woerly, E. M.; Roy, J.; Burke, M. D. *Nat. Chem.* **2014**, *6*, 484. (b) Hopf, H. *Classics in Hydrocarbon Chemistry: Syntheses, Concepts, Perspectives*; Wiley-VCH: Weinheim, 2000; pp 103–112.
- (18) Nicolaou, K. C.; Sorensen, E. J. *Classics in Total Synthesis: Targets, Strategies, Methods*, 1st ed.; VCH: Weinheim, 1996.
- (19) (a) Hückel, E. *Z. Eur. Phys. J. A* **1931**, *70*, 204. (b) Hückel, E. *Z. Eur. Phys. J. A* **1931**, *72*, 310. (c) Hückel, E. *Z. Eur. Phys. J. A* **1932**, *76*, 628.
- (20) Spittler, E. L.; Johnson, C. A.; Haley, M. M. *Chem. Rev.* **2006**, *106*, 5344.
- (21) (a) Boese, R.; Weiss, H.-C.; Bläser, D. *Angew. Chem., Int. Ed.* **1999**, *38*, 988. (b) Thalladi, V. R.; Boese, R.; Weiss, H.-C. *J. Am. Chem. Soc.* **2000**, *122*, 1186. (c) Thalladi, V. R.; Nüsse, M.; Boese, R. *J. Am. Chem. Soc.* **2000**, *122*, 9227. (d) van Langevelde, A.; Peschar, R.; Schenk, H. *Chem. Mater.* **2001**, *13*, 1089. (e) White, N. A. S.; Ellis, H. A.; Nelson, P. N.; Maragh, P. T. *J. Chem. Thermodyn.* **2011**, *43*, 584. (f) Ramin, L.; Jabbarzadeh, A. *Langmuir* **2011**, *27*, 9748. (g) Nelson, P. N.; Ellis, H. A.; Taylor, R. A. *J. Mol. Struct.* **2011**, *986*, 10. (h) Nelson, P. N.; Ellis, H. A. *Dalton Trans.* **2012**, *41*, 2632. (i) Bhattacharya, S.; Saraswatula, V. G.; Saha, B. K. *Cryst. Growth Des.* **2013**, *13*, 3651. (j) de la Rama, L. P.; Hu, L.; Ye, Z.; Efremov, M. Y.; Allen, L. H. *J. Am. Chem. Soc.* **2013**, *135*, 14286. (k) Nelson, P. N.; Ellis, H. A. *J. Mol. Struct.* **2014**, *1075*, 299.
- (22) Improved syntheses of [7]dendralene and [8]dendralene involving lynchpin approaches are described in the SI.
- (23) Jacobsen, E. N.; Bergman, R. G. *J. Am. Chem. Soc.* **1985**, *107*, 2023.
- (24) (a) Reich, H. J.; Yelm, K. E.; Reich, I. L. *J. Org. Chem.* **1984**, *49*, 3438. (b) Wille, F.; Dirr, K.; Kerber, H. *Justus Liebigs Ann. Chem.* **1955**, *591*, 177. (c) Sajadi, S. A. A.; Pruhan, G. H.; Mostaghim, R. *Nashrieh Shimi va Mohandesi Shimi Iran* **2003**, *22*, 39.
- (25) (a) Hata, T.; Kitagawa, H.; Masai, H.; Kurahashi, T.; Shimizu, M.; Hiyama, T. *Angew. Chem., Int. Ed.* **2001**, *40*, 790. (b) Kurahashi, T.; Hata, T.; Masai, H.; Kitagawa, H.; Shimizu, M.; Hiyama, T. *Tetrahedron* **2002**, *58*, 6381.
- (26) (a) Shimizu, M.; Kurahashi, T.; Hiyama, T. *Synlett* **2001**, *SI*, 1006. (b) Shimizu, M.; Kurahashi, T.; Shimono, K.; Tanaka, K.; Nagao, I.; Kiyomoto, S.-I.; Hiyama, T. *Chem. - Asian J.* **2007**, *2*, 1400.
- (27) (a) Gavryushin, A.; Kofink, C.; Manolikakes, G.; Knochel, P. *Tetrahedron* **2006**, *62*, 7521. (b) Barluenga, J.; Moriel, P.; Aznar, F.; Valdés, C. *Adv. Synth. Catal.* **2006**, *348*, 347. (c) Bojase, G.; Payne, A. D.; Willis, A. C.; Sherburn, M. S. *Angew. Chem., Int. Ed.* **2008**, *47*, 910. (d) Kohnen, A. L.; Danheiser, R. L. *Org. Synth.* **2007**, *84*, 77. (e) Kottirsch, G.; Szeimies, G. *Chem. Ber.* **1990**, *123*, 1495.
- (28) Shimizu, M.; Tanaka, K.; Kurahashi, T.; Shimono, K.; Hiyama, T. *Chem. Lett.* **2004**, *33*, 1066.
- (29) (a) Yamamoto, T.; Yasuda, T.; Kobayashi, K.; Yamaguchi, I.; Koizumi, T.-A.; Ishii, D.; Nakagawa, M.; Mashiko, Y.; Shimizu, N. *Bull.*

Chem. Soc. Jpn. **2006**, *79*, 498. (b) Hopf, H.; Theurig, M. *Angew. Chem., Int. Ed. Engl.* **1994**, *33*, 1099.

(30) For a summary of reaction conditions examined, see SI.

(31) (a) Rahimi, A.; Schmidt, A. *Synthesis* **2010**, *2010*, 2621. (b) Chelucci, G.; Capitta, F.; Baldino, S. *Tetrahedron* **2008**, *64*, 10250.

(c) Chelucci, G.; Capitta, F.; Baldino, S.; Pinna, G. A. *Tetrahedron Lett.* **2007**, *48*, 6514. (d) Jacobsen, M. F.; Moses, J. E.; Adlington, R. M.; Baldwin, J. E. *Org. Lett.* **2005**, *7*, 641. (e) Jacobsen, M. F.; Moses, J. E.; Adlington, R. M.; Baldwin, J. E. *Tetrahedron* **2006**, *62*, 1675. (f) Yan, H.; Lu, L.; Sun, P.; Zhu, Y.; Yang, H.; Liu, D.; Rong, G.; Mao, J. *RSC Adv.* **2013**, *3*, 377. (g) Liu, J.; Dai, F.; Yang, Z.; Wang, S.; Xie, K.; Wang, A.; Chen, X.; Tan, Z. *Tetrahedron Lett.* **2012**, *53*, 5678. (h) Shen, W.; Wang, L. *J. Org. Chem.* **1999**, *64*, 8873. (i) Zapata, A. J.; Ruíz, J. *J. Organomet. Chem.* **1994**, *479*, C6.

(32) Sondheimer, F.; Ben-Efraim, D. A.; Wolovsky, R. *J. Am. Chem. Soc.* **1961**, *83*, 1675.

(33) Williams, D. H.; Fleming, I. *Spectroscopic Methods in Organic Chemistry*, 3rd ed.; McGraw-Hill: London, 1980; pp 6–11.

(34) The magnitudes of extinction coefficients for [5]dendralene and [7]dendralene reported in our 2009 study (see ref 8) are slightly different to those reported here.

(35) By ¹H NMR spectroscopic analysis, the product ratio of the monoadducts is ca. 85:15 (*terminal/internal* monoadduct). This ratio is reversed in [4]dendralene. A similar analysis of the bis-adducts shows a ca. 75% preference for the *terminal/terminal* regioisomer. The *terminal/internal* regioisomer dominates with [4]dendralene (65% selectivity).

(36) (a) Curtiss, L. A.; Redfern, P. C.; Raghavachari, K. *J. Chem. Phys.* **2007**, *126*, 084108. (b) Curtiss, L. A.; Redfern, P. C.; Raghavachari, K. *J. Chem. Phys.* **2007**, *127*, 124105.

(37) (a) Herrebout, W. A.; van der Veken, B. J.; Wang, A.; Durig, J. R. *J. Phys. Chem.* **1995**, *99*, 578. (b) Pratt, L. R.; Hsu, C. S.; Chandler, D. *J. Chem. Phys.* **1978**, *68*, 4202.

(38) Almenningen, A.; Gatjal, A.; Grace, D. S. B.; Hopf, H.; Klæboe, P.; Lehrich, F.; Nielsen, C. J.; Powell, D. L.; Trættemberg, M. *Acta Chem. Scand.* **1988**, *42*, 634.

(39) Palmer, M. H.; Blair-Fish, J. A.; Sherwood, P. *J. Mol. Struct.* **1997**, *412*, 1.

(40) Lodewyk, M. W.; Soldi, C.; Jones, P. B.; Olmstead, M. M.; Rita, J.; Shaw, J. T.; Tantillo, D. J. *J. Am. Chem. Soc.* **2012**, *134*, 18550.

(41) Chai, J.-D.; Head-Gordon, M. *J. Chem. Phys.* **2008**, *128*, 084106.

(42) Paddon-Row, M. N.; Sherburn, M. S. *Chem. Commun.* **2012**, *48*, 832.